Biophysical Chemistry, 48 (1993) 193–204
Elsevier Science Publishers B.V., Amsterdam

BIOCHE 01808

Fluorescence quenching by metal ions in lipid bilayers

A.S. Holmes, K. Suhling and D.J.S. Birch *

Department of Physics and Applied Physics, University of Strathclyde, Glasgow (UK)

(Received 25 May 1993; accepted in revised form 23 August 1993)

Abstract

Fluorescence quenching of perylene by Co^{2+} and Ni^{2+} ions has been investigated both below and above the phase transition temperature in small unilamellar DPPC vesicles. Classic Förster type energy transfer was observed for perylene quenched by Co^{2+} ions below the phase transition when the effects of donor–donor energy transfer are taken into account. In the liquid crystalline phase a simple diffusion theory incorporating energy transfer was found to model the system well. For quenching by Ni^{2+} ions both above and below the phase transition temperature in lipid bilayers and in glycerol the data did not follow classic Förster type energy transfer but indicated that an additional quenching mechanism was present. A mechanism other than Förster behaviour was also observed for the quenching by Cr^{3+} ions in glycerol.

Keywords: Energy transfer; Perylene; Metal ions; Lipid bilayers

1. Introduction

Fluorescence probe techniques are now well established in the study of membranes and other ordered media [1]. The quenching of aromatic fluorescence by metal ions can involve a number of mechanisms including electron transfer, Dexter electron exchange, heavy atom induced intersystem crossing, exciplex formation and Förster energy transfer. Energy transfer studies in ordered media are singularly useful in describing the locations of both donors and acceptors, which are usually both aromatic molecules. An alternative approach, which we have been developing and will report here, is to use transition metal ions as acceptors [2,3]. Most fluorescence quenching studies in heterogeneous media have to date been in micellar solutions where, for example, the quenching of pyrene by metal ions [4–7] has been reported.

Many of the transition metal ions like Co^{2+}, Ni^{2+} and Cr^{3+} are useful in the context of non-radiative energy transfer as their absorption spectra in solution show good overlap with many of the widely used aromatic probes. The lack of radiative emission from such ions is a further advantage over using aromatic acceptors. In aqueous solution cobalt, nickel and chromium exist as the hexaaquo ions $[Co \cdot 6H_2O]^{2+}$, $[Ni \cdot 6H_2O]^{2+}$ and $[Cr \cdot 6H_2O]^{3+}$. Therefore in membranes we would expect these to be bound to the anionic lipid headgroup. Such site-specific location is a further useful property of metal ion acceptors. As a non-polar, nearly disk-shaped

* Corresponding author.

molecule perylene is thought to lie within the hydrocarbon region of a bilayer. The fluorescence properties of perylene are well documented both in homogeneous solutions [8] and lipid bilayers [9]. In summary, the perylene-transition metal ion interaction is a relatively well defined problem.

Theoretical expressions to describe dipole–dipole energy transfer in homogeneous media were first developed by Förster [10] and then by various authors in the regions where Förster's theory breaks down [11–19]. Förster's model [10] only being strictly valid for negligible diffusion at low donor and high acceptor concentrations. The models proposed by Huber [11,12] and Loring et al. [15] (LAF) are valid in the region where the donor–acceptor energy transfer is slow in comparison to the donor–donor energy transfer and diffusion is absent. Huber's work is a restricted case of the LAF theory. These models have been verified experimentally in solution by Pandey et al. [20] and shown to be still useful in lipid bilayers [21]. When diffusion is occurring the models proposed by Gösele et al. [16,17] provide a simple and reasonable approximation. Two models are available depending on the extent to which diffusion is influencing the energy transfer [16,17]. These models have been used experimentally by Tamai et al. [22] and Pandey and Pant [23] to describe diffusion controlled energy transfer between rhodamine 6G and malachite green and between acriflavine and rhodamine 6G, respectively.

Recently we have reported the quenching of perylene fluorescence by Co^{2+} ions in glycerol as being well described by Förster long-range dipole–dipole energy transfer with an interaction radius of 13.2 Å [24]. However, in lipid bilayers a complication arises in the kinetics due to perylene-perylene dipole–dipole energy transfer as a consequence of clustering of the perylene molecules [21]. Another quenching mechanism has been observed for perylene fluorescence quenched by Ag^{2+} ions, where an exciplex was formed [25,26]. Here we compare and contrast the quenching mechanisms for the perylene fluorescence with the transition metal ions cobalt, nickel and chromium in glycerol and the former two metal ions in small unilamellar vesicles of L-α-dipalmitoylphosphatidylcholine (DPPC) below and above the phase transition.

2. Kinetic models

For the case of dipole–dipole resonance energy transfer in the absence of diffusion, Förster's theory gives the fluorescence response function as [10]

$$I(t) = I_0 \exp\left(\frac{-t}{\tau_0} - 2\gamma\left(\frac{t}{\tau_0}\right)^{d/6}\right) \qquad (1)$$

where d describes the dimensionality such that $d = 3$ for three-dimensional (3D) Förster energy transfer and $d = 2$ for 2D energy transfer, τ_0 is the lifetime of the unquenched donor and $\gamma = [A]/C_{AO}$ with [A] the acceptor concentration and C_{AO} the critical acceptor concentration for energy transfer.

The critical transfer distance R_0 can be expressed by the following equation

$$R_0^6 = \frac{9\ln(10)K^2\phi_0}{128\pi^5 N_A n^4}\int_0^\infty \frac{F_d(\tilde{\nu})\epsilon_a(\tilde{\nu})}{(\tilde{\nu})^4}\,d(\tilde{\nu}) \qquad (2)$$

Here ϕ_0 is the emission quantum yield of the donor in absence of the acceptor, K is the orientation factor and n is the refractive index of the solvent. $F_d(\tilde{\nu})$ is the emission intensity of the donor and $\epsilon_a(\tilde{\nu})$ is the extinction coefficient of the acceptor at the wavenumber $\tilde{\nu}$. The orientation factor, K^2, is equal to 0.67 for donor and acceptor molecules which rotate freely and rapidly relative to the fluorescence lifetime of the donor. This is the case above the phase transition in the lipid but not below where the perylene motion is restricted [9]. However, when either the donor or acceptor molecule is free to rotate, as is the case here with the Co^{2+} ions, then the extreme values for K^2 are 1.33 and 0.33 resulting in a maximum error in R_0 due to assuming $K^2 = 0.67$ of approximately 12% [27,28]. The critical concentration C_{AO} is related to R_0 by

$$C_{AO} = \frac{3}{2\pi^{3/2} N_A R_0^3} \qquad (3)$$

When the rate of energy transfer from donor–donor is comparable to that from donor–acceptor, then the donor fluorescence decay is more appropriately described by a modified form of the Förster equation as proposed by Huber [11,12]:

$$I(t) = I_0 \exp\left(-\frac{t}{\tau_0} - \left(\sqrt{2}\,\gamma_D + 2\gamma_A\right)\left(\frac{t}{\tau_0}\right)^{d/6}\right) \tag{4}$$

where the subscripts D and A refer to donor and acceptor respectively. The reversible migration of energy among the donor molecules is accounted for by the reduced factor for the donor transfer [11].

When the effects of diffusion are also present in the system as well as energy transfer then the expressions given by Gösele et al. [16,17] are more appropriate. There are two forms of the donor decay depending on the extent to which diffusion is influencing the energy transfer kinetics. They are

$$I(t) = I_0 \exp\left(-\frac{t}{\tau_0} - 4\pi D r_F [A] N_A t - 2\gamma\left(\frac{t}{\tau_0}\right)^{1/2}\right) \tag{5}$$

for $r_F/r_{AD} > 1$

and

$$I(t) = I_0 \exp\left(-\frac{t}{\tau_0} - 4\pi D r_{AD} [A] N_A t - 8 r_{AD}^2 [A] N_A (\pi D t)^{1/2}\right) \tag{6}$$

for $r_F/r_{AD} < 1$

where r_{AD} is the collision radius where immediate energy transfer is assumed to occur and r_F is an effective trapping radius given by

$$r_F \approx 0.676\left(\frac{R_0^6}{\tau_0 D}\right)^{1/4} \tag{7}$$

where $D = D_D + D_A$ is the sum of the donor and acceptor diffusion coefficients.

In a high viscosity solvent, where the diffusion length of the donor and acceptor is much shorter than the critical transfer distance, then equation (5) can be simplified to Förster's model which is given in eq. (1). Equation (6) is analogous to the Smoluchowski expression for pure diffusion controlled reactions where no long range energy transfer is present.

The relative donor quantum yield for Förster energy transfer can be expressed as [1]

$$\phi/\phi_0 = 1 - \pi^{1/2}\gamma \exp(\gamma^2)\,\mathrm{erfc}(\gamma) \tag{8}$$

where erfc is the complementary error function. At small quencher concentrations eq. (8) reduces to

$$\phi/\phi_0 = 1 - \pi^{1/2}\gamma \tag{9}$$

At shorter ranges of interaction (i.e. < 10 Å) than that over which Förster energy transfer is dominant electron exchange interactions and higher multipole–multipole interactions can become dominant, particularly when dipole–dipole interactions are forbidden. The principle requirement for such so called Dexter electron exchange is overlap of the excited donor and acceptor molecular orbitals [29]. A specific feature of the Dexter mechanism is that unlike the Förster mechanism the energy transfer rate is independent of oscillator strength of the acceptor transition, which in the case of Ni^{2+}, we have measured to be ≈ 2–3 times less than for Co^{2+}.

Distinguishing between Förster and Dexter energy transfer is often not readily achieveable at short distances of interaction and has been little explored by comparing the fit of the fluorescence decay to the appropriate impulse responses. In contrast to eq. (8) describing Förster kinetics the equivalent expression for Dexter kinetics is of the form [30]

$$\phi/\phi_0 = \exp(-[A]/C_{AO}) \tag{10}$$

Hence the shape of ϕ/ϕ_0 vs. [A] provides, in theory at least, one method of distinguishing between the two kinetics.

3. Experimental

Perylene (Aldrich Gold Label), glycerol (Aldrich), $NiCl_2 \cdot 6H_2O$ (Aldrich) and $CrCl_3 \cdot 6H_2O$ (BDH) were used as received. $CoCl_2 \cdot 6H_2O$ (Merck p.a.) was recrystallized from methanol. L-α-dipalmitoylphosphatidylcholine (DPPC) was obtained from the Sigma Chemical Co.

Small unilammelar vesicles (SUV) were prepared using methanol injection at 328 K which is above the phase transition temperature for DPPC ($T_M = 314$ K). The lipid-to-probe ratio in all cases was 200:1. The concentration of the lipid in the buffer was 6.18×10^{-4} mol l^{-1}. The buffer solution was piperazine-*N*,*N*′-bis-2-ethane-sulfonic acid (PIPES) (Biochemical BDH) with KCl (Aldrich) and EDTA (Alrich). Sodium azide (Aldrich) was added to obtain a pH of 7 [31].

Fluorescence spectra were recorded with either a Perkin-Elmer MPF-44 E spectrofluorimeter with a quantum correction unit or a Shimadzu RF-540 spectrofluorimeter. Both instruments were fitted with a thermostated cuvette holder. All fluorescence spectra were corrected for reabsorption of the metal ion complexes, using the method of Marciniak [32].

Fluorescence decay kinetics were measured using the technique of time-correlated single photon counting [33]. Either the coaxial flashlamp filled with hydrogen or a Hamamatsu PLP-01 frequency doubled diode laser operated at 10 MHz repetition rate was used for excitation. Operating the lamp at 40 kHz gives an instrumental pulse ~ 1.5 ns FWHM. The diode laser gave an instrumental pulse width of ≈ 350 ps FWHM. The excitation wavelength for all measurements was 385 nm. Prism polarisers were used at the "magic angle" to eliminate rotational effects. The sample temperature was controlled by electrical heating (Eurotherm) with a precision of ±0.5 K. The maximum number of counts in a channel was between 1×10^4 and 2×10^4 recorded at channel

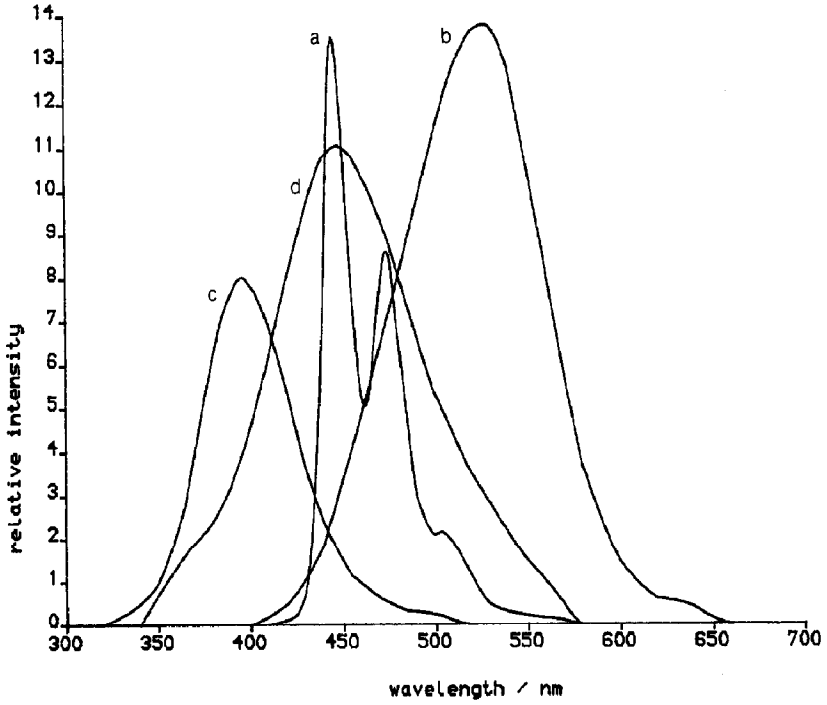

Fig. 1. Fluorescence spectrum for perylene in lipid bilayers (a) and the absorption spectra for Co^{2+} (b) and Ni^{2+} (c) ions bound to the lipid headgroup at $T = 303$ K, and for Cr^{3+} (d) ions in glycerol.

widths down to 84 ps/ch. Data analysis was performed using the IBH iterative reconvolution library.

4. Results and discussion

The fluorescence spectrum for perylene in DPPC bilayers and the absorption spectra for Co^{2+} and Ni^{2+} ions bound to the lipid headgroup at $T = 303$ K are shown in Fig 1. Also shown in Fig. 1 is the absorption spectrum for Cr^{3+} ions in glycerol which has the biggest overlap with the perylene fluorescence spectra. The Co^{2+} and Ni^{2+} absorption spectra can be seen to be on the low and high energy side of the perylene emission spectrum respectively. In the case of Ni^{2+} significantly more overlap with the perylene absorption is observed. Addition of metal ions to the vesicles did not affect their stability as a single phase transition at $T = 314$ K was observed at all metal ion concentrations.

In small unilamellar DPPC vesicles in the gel phase ($T = 303$ K) the fluorescence lifetime of perylene is 6.31 ns with a χ^2 of 1.31 and hence shows small deviations from a single exponential function. This we attributed to the effects of donor–donor energy transfer due to clustering of the perylene molecules in the gel phase [21]. The non-random distribution of probe molecules was observed in perylene concentration studies of the lipid bilayer [21] which showed no evidence for the formation of perylene dimers from the steady state spectra. Also, analysing the fluorescence decay at different emission wavelengths gave the same results confirming that perylene dimers are not formed and that the quenching mechanism is Förster type energy transfer. From these studies it was evident that the number of perylene molecules involved in the energy transfer processes is independent of the size of the perylene cluster once the minimum number of molecules were present for the donor–donor energy transfer process to occur [21]. When increasing the temperature to 323 K (i.e. the liquid crystalline phase), the fluorescence decay function can be fitted better to a monoexponential fit ($\chi^2 = 1.09$) with a reduced lifetime of 5.81 ns. In this phase the bilayer becomes more fluid and the volume is increased which results in the perylene molecule having more mobility and hence probe clustering will be reduced [34]. The fluorescence lifetimes measured here are in agreement with those reported in DMPC and DOPC vesicles [9,35].

4.1. Perylene–cobalt studies

When $CoCl_2 \cdot 6H_2O$ is added to the liposome suspension the fluorescence decay curves cannot be fitted to a monoexponential decay law. The deviations being significantly higher below the phase transition (T_M). The stronger quenching effect above T_M is evident from the faster fluorescence decay. At $[Co^{2+}] = 0.1$ mol l^{-1}, the mean lifetimes calculated from $\tau_e = \int_0^\infty tI(t)dt / \int_0^\infty I(t)dt$ are τ_e (303 K) = 3.80 ns and τ_e (323 K) = 3.29 ns. In the lipid bilayer the cobalt ions are anchored at the lipid headgroup with an

Table 1

Best-fit parameters at 303 K to a 3D Förster fit and values calculated for R_0 from eq. (4) for the fluorescence quenching of perylene at different Co^{2+}-ion concentrations in DPPC vesicles

Co^{2+} (mol l^{-1})	τ_0/ns	Förster kinetics 3D model parameter			Equation (4)	
		γ	χ^2_{3D}	R_0/Å	γ_A	R_0/Å
0.011	6.60 ± 0.21	0.138	1.25	17.7 ± 0.3	0.053	12.9 ± 1.0
0.021	6.45 ± 0.21	0.208	1.05	16.4 ± 0.2	0.123	13.8 ± 0.5
0.031	6.38 ± 0.24	0.299	1.22	16.3 ± 0.3	0.214	14.6 + 0.3
0.041	6.37 ± 0.24	0.352	1.13	15.7 ± 0.1	0.267	14.3 ± 0.3
0.060	5.95 ± 0.24	0.392	1.18	14.3 ± 0.1	0.307	13.2 ± 0.2
0.080	5.96 ± 0.27	0.430	1.23	13.4 ± 0.1	0.345	12.4 ± 0.2
0.100	6.15 ± 0.30	0.529	1.30	13.3 ± 0.1	0.444	12.6 + 0.2

ion-lipid binding constant for Co^{2+} and DPPC of 1.71 mol^{-1} [36]. Even at the lowest Co^{2+} concentration of 0.01 mol l^{-1} of cobalt chloride the Co^{2+} : lipid ratio is 12.5 : 1. Hence the metal ion concentration at the lipid headgroup is high.

Below the phase transition temperature (i.e. in the gel phase) diffusional effects are minimal, hence we have analysed the data in terms of Förster kinetics for both a three dimensional and a two dimensional representation. Intuitively a two dimensional model may appear to be more appropriate for the lipid system that we are studying given that the cobalt ions are bound to the lipid headgroup and the perylene molecules are within the interior of the bilayer. However, the χ^2 values are consistently better for the three-dimensional description and the values obtained for γ are similar for both models. Hence we have calculated values for the interaction radius, R_0, from eqs. (1) and (3) and these are given in Table 1. The values obtained for R_0 calculated for a two-dimensional model, are, within the error, the same as those calculated assuming a 3D system. Below T_M the values obtained for R_0 are not constant as expected but are too high at the low acceptor concentrations (i.e. for $[CoCl_2 \cdot 6H_2O] \leq 0.06$ mol l^{-1}). The value for R_0 calculated from the overlap of the absorption spectra of $CoCl_2 \cdot 6H_2O$ and the emission spectra of perylene using eq. (2) is 13.9 Å in the lipid bilayer and 12.4 Å in glycerol. The difference between the two values is due to the spectral shift of the Co^{2+} ion absorption. The experimental value for R_0 in glycerol solution is 13.4 Å [24]. Also, the plot of γ versus $[Co^{2+}]$ (Fig. 2) gives a value for R_0 of 12.1 ± 1.6 Å from the slope but does not go through the origin as predicted by eq. (3). This suggests that an additional energy transfer process is occurring at the low acceptor concentrations. This was found to be donor–donor energy transfer between the perylene molecules, as the rate of donor–donor energy transfer is comparable to the rate of donor–acceptor energy transfer [21]. Radiative energy transfer was excluded as no evidence was found for this in the steady state spectra. Analysing the perylene fluorescence decay with no quencher added in terms of Förster kinetics (eq. (1)) gave a

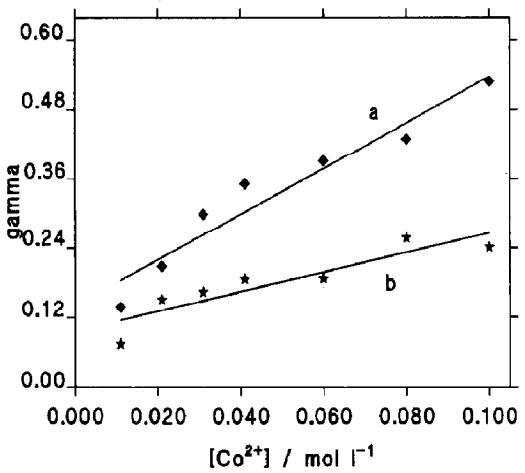

Fig. 2. Plot of γ vs. $[Co^{2+}]$ for perylene–cobalt energy transfer in lipid bilayers at (a) 303 K. and (b) 323 K.

value for γ_D of 0.120 ± 0.006 which is, within the error, consistent with the intercept of the straight line graph in Fig. 2 i.e. 0.140 ± 0.038. Given this value for γ_D we can analyse the fluorescence decays using eq. (4), which takes the effects of donor–donor energy transfer into account. The values obtained for R_0 (see Table 1) were then found to be constant with a mean value of 13.4 Å, in good agreement with the R_0 measured in glycerol and calculated from eq. (2).

Table 2 gives the parameters obtained when using Förster's model for a 3D system (eq. 1) to

Table 2

Best-fit parameters at 323 K to a 3D Förster fit and values calculated for R_0, taking donor–donor energy transfer into account, and D from eq. (5) for the fluorescence quenching of perylene at different Co^{2+}-ion concentrations in DPPC vesicles

Co^{2+} (mol l^{-1})	Förster kinetics 3D model parameters			R_0/Å	$D/10^{-6}$ cm^2 s^1
	τ_0/ns	γ	χ^2		
0.011	5.41±0.15	0.074	1.05	11.2±1.4	1.20±0.08
0.021	5.18±0.16	0.151	1.10	13.4±0.6	0.92±0.04
0.031	5.01±0.16	0.164	1.06	12.2±0.5	0.92±0.04
0.041	4.85±0.18	0.186	1.19	11.7±0.4	0.98±0.03
0.060	4.48±0.17	0.187	1.13	10.3±0.3	1.31±0.05
0.080	4.47±0.20	0.258	1.22	10.7±0.3	0.90±0.02
0.100	4.18±0.18	0.241	1.15	9.7±0.3	1.15±0.02

describe the fluorescence decay data above the phase transition temperature of the lipid. Once again the model of a 3D system was found to be more appropriate, as judged by the χ^2 values, but both the 2D and 3D models give similar γ and τ_0 values. Here the values obtained for τ_0 decrease significantly with increasing Co^{2+} concentration reflecting the diffusion of the perylene molecules and cobalt ions as might be expected in the liquid crystalline phase of the lipid bilayer. Below T_M the fluorescence lifetime, τ_0, is almost constant showing that little diffusion occurs in the gel phase (see Table 1).

We have therefore considered the expressions given by Gösele et al. [16,17] for diffusion controlled energy transfer (eqs. 5 and 6) in the liquid crystalline phase. To decide which is the more appropriate expression in our case we calculated r_F and r_{AD} from our experimental data. For $[Co^{2+}] = 0.061$ mol l^{-1}, we calculated $r_F = 8.6$ Å, from eqs. (5) and (7), and $r_{AD} = 4.4$ Å, from eq. (6), which then gives for the ratio r_F/r_{AD} a value of 1.95, indicating that eq. (5) is more appropriate and energy transfer dominates over diffusion. This is not the case in the solvent ethylene glycol where $r_F/r_{AD} < 1$ which shows that in this solvent the quenching of perylene fluorescence by cobalt ions is purely diffusion controlled as already reported [24].

The parameters obtained from interpreting the fluorescence decay data in the liposome above T_M, using eq. (5), are given in Table 2. The results show evidence for donor–donor energy transfer between the perylene molecules above the phase transition similar to that observed in the gel phase. When plotting γ versus $[Co^{2+}]$ the straight line graph does not go through the origin (Fig. 2). The critical transfer distance R_0 calculated from the gradient of this graph is 9.9 ± 1.8 Å which is less, although within the error of that observed below the phase transition where R_0 is calculated to be 12.1 ± 1.6 Å. Taking the data set with no quencher added and analysing in terms of Förster's model (eq. 1) gives $\gamma = 0055 \pm 0.006$ and $\tau_0 = 6.09$ ns. This γ value is close to the intercept of the graph in Fig. 2 (0.090 ± 0.029) consistent with the presence of donor–donor energy transfer above the phase transition.

Once again the occurrence of donor–donor energy transfer provides interesting evidence for there being clustering of the probe molecules. It is notable that this occurs above as well as below the phase transition. A 200:1 lipid-to-probe ratio corresponds to an equivalent molar concentration of $\approx 10^{-2}M$ and yet even in the same concentration in a homogeneous solution of perylene molecules, where self-absorption is the more predominant process, radiationless energy transfer between the perylene molecules is not evident as the fluorescence decays can be fitted well to a monoexponential fit albeit with an increased lifetime due to self absorption. However, this may not be surprising given that the mean separation between perylene molecules at this concentration is ≈ 55 Å and the Förster energy transfer radius is 35.7 Å [21]. This provides further supporting evidence for the non-random distribution of perylene molecules in the fluid phase of the bilayer. However, the perylene clusters need not be tightly bound in order for Förster energy transfer to occur. Indeed, the non-exponentiality of the fluorescence decay of other fluorophores in lipid bilayers, especially in the gel phase, may have their origin in inter fluorophore interactions such as energy transfer processes due to the non random distribution of fluorophores.

Above the phase transition the diffusion of both the donor and acceptor molecules as well as energy transfer from donor to donor and also acceptor presents a complex kinetic system. We should emphasise that in the treatment we are using the evidence points to donor–donor interactions appearing as two terms, namely Förster energy transfer as if static conditions prevailed and also diffusion of the donor sites. In such cases a diffusion term in the donor rate equation is also needed for describing the donor–donor energy transfer, this term not being required below the phase transition. Gochanour et al. [14] have derived an approximate expression to account for this behaviour in terms of the excitation diffusion coefficient, D_E, which is valid at long times and high donor concentrations and is given by

$$D_E = 0.428 C^{4/3} R_{0D}^2 \tau_0^{-1} \qquad (11)$$

molecule perylene is thought to lie within the hydrocarbon region of a bilayer. The fluorescence properties of perylene are well documented both in homogeneous solutions [8] and lipid bilayers [9]. In summary, the perylene-transition metal ion interaction is a relatively well defined problem.

Theoretical expressions to describe dipole–dipole energy transfer in homogeneous media were first developed by Förster [10] and then by various authors in the regions where Förster's theory breaks down [11–19]. Förster's model [10] only being strictly valid for negligible diffusion at low donor and high acceptor concentrations. The models proposed by Huber [11,12] and Loring et al. [15] (LAF) are valid in the region where the donor–acceptor energy transfer is slow in comparison to the donor–donor energy transfer and diffusion is absent. Huber's work is a restricted case of the LAF theory. These models have been verified experimentally in solution by Pandey et al. [20] and shown to be still useful in lipid bilayers [21]. When diffusion is occurring the models proposed by Gösele et al. [16,17] provide a simple and reasonable approximation. Two models are available depending on the extent to which diffusion is influencing the energy transfer [16,17]. These models have been used experimentally by Tamai et al. [22] and Pandey and Pant [23] to describe diffusion controlled energy transfer between rhodamine 6G and malachite green and between acriflavine and rhodamine 6G, respectively.

Recently we have reported the quenching of perylene fluorescence by Co^{2+} ions in glycerol as being well described by Förster long-range dipole–dipole energy transfer with an interaction radius of 13.2 Å [24]. However, in lipid bilayers a complication arises in the kinetics due to perylene-perylene dipole–dipole energy transfer as a consequence of clustering of the perylene molecules [21]. Another quenching mechanism has been observed for perylene fluorescence quenched by Ag^{2+} ions, where an exciplex was formed [25,26]. Here we compare and contrast the quenching mechanisms for the perylene fluorescence with the transition metal ions cobalt, nickel and chromium in glycerol and the former two metal ions in small unilamellar vesicles of L-α-dipalmitoylphosphatidylcholine (DPPC) below and above the phase transition.

2. Kinetic models

For the case of dipole–dipole resonance energy transfer in the absence of diffusion, Förster's theory gives the fluorescence response function as [10]

$$I(t) = I_0 \exp\left(\frac{-t}{\tau_0} - 2\gamma\left(\frac{t}{\tau_0}\right)^{d/6}\right) \qquad (1)$$

where d describes the dimensionality such that $d = 3$ for three-dimensional (3D) Förster energy transfer and $d = 2$ for 2D energy transfer, τ_0 is the lifetime of the unquenched donor and $\gamma = [A]/C_{AO}$ with [A] the acceptor concentration and C_{AO} the critical acceptor concentration for energy transfer.

The critical transfer distance R_0 can be expressed by the following equation

$$R_0^6 = \frac{9\ln(10)K^2\phi_0}{128\pi^5 N_A n^4}\int_0^\infty \frac{F_d(\tilde{\nu})\epsilon_a(\tilde{\nu})}{(\tilde{\nu})^4}\,d(\tilde{\nu}) \qquad (2)$$

Here ϕ_0 is the emission quantum yield of the donor in absence of the acceptor, K is the orientation factor and n is the refractive index of the solvent. $F_d(\tilde{\nu})$ is the emission intensity of the donor and $\epsilon_a(\tilde{\nu})$ is the extinction coefficient of the acceptor at the wavenumber $\tilde{\nu}$. The orientation factor, K^2, is equal to 0.67 for donor and acceptor molecules which rotate freely and rapidly relative to the fluorescence lifetime of the donor. This is the case above the phase transition in the lipid but not below where the perylene motion is restricted [9]. However, when either the donor or acceptor molecule is free to rotate, as is the case here with the Co^{2+} ions, then the extreme values for K^2 are 1.33 and 0.33 resulting in a maximum error in R_0 due to assuming $K^2 = 0.67$ of approximately 12% [27,28]. The critical concentration C_{AO} is related to R_0 by

$$C_{AO} = \frac{3}{2\pi^{3/2} N_A R_0^3} \qquad (3)$$

When the rate of energy transfer from donor–donor is comparable to that from donor–acceptor, then the donor fluorescence decay is more appropriately described by a modified form of the Förster equation as proposed by Huber [11,12]:

$$I(t) = I_0 \exp\left(-\frac{t}{\tau_0} - \left(\sqrt{2}\,\gamma_D + 2\gamma_A\right)\left(\frac{t}{\tau_0}\right)^{d/6}\right) \tag{4}$$

where the subscripts D and A refer to donor and acceptor respectively. The reversible migration of energy among the donor molecules is accounted for by the reduced factor for the donor transfer [11].

When the effects of diffusion are also present in the system as well as energy transfer then the expressions given by Gösele et al. [16,17] are more appropriate. There are two forms of the donor decay depending on the extent to which diffusion is influencing the energy transfer kinetics. They are

$$I(t) = I_0 \exp\left(-\frac{t}{\tau_0} - 4\pi D r_F [A] N_A t - 2\gamma\left(\frac{t}{\tau_0}\right)^{1/2}\right) \tag{5}$$

for $r_F/r_{AD} > 1$

and

$$I(t) = I_0 \exp\left(-\frac{t}{\tau_0} - 4\pi D r_{AD} [A] N_A t - 8 r_{AD}^2 [A] N_A (\pi D t)^{1/2}\right) \tag{6}$$

for $r_F/r_{AD} < 1$

where r_{AD} is the collision radius where immediate energy transfer is assumed to occur and r_F is an effective trapping radius given by

$$r_F \approx 0.676\left(\frac{R_0^6}{\tau_0 D}\right)^{1/4} \tag{7}$$

where $D = D_D + D_A$ is the sum of the donor and acceptor diffusion coefficients.

In a high viscosity solvent, where the diffusion length of the donor and acceptor is much shorter than the critical transfer distance, then equation (5) can be simplified to Förster's model which is given in eq. (1). Equation (6) is analogous to the Smoluchowski expression for pure diffusion controlled reactions where no long range energy transfer is present.

The relative donor quantum yield for Förster energy transfer can be expressed as [1]

$$\phi/\phi_0 = 1 - \pi^{1/2}\gamma \exp(\gamma^2)\,\mathrm{erfc}(\gamma) \tag{8}$$

where erfc is the complementary error function. At small quencher concentrations eq. (8) reduces to

$$\phi/\phi_0 = 1 - \pi^{1/2}\gamma \tag{9}$$

At shorter ranges of interaction (i.e. < 10 Å) than that over which Förster energy transfer is dominant electron exchange interactions and higher multipole–multipole interactions can become dominant, particularly when dipole–dipole interactions are forbidden. The principle requirement for such so called Dexter electron exchange is overlap of the excited donor and acceptor molecular orbitals [29]. A specific feature of the Dexter mechanism is that unlike the Förster mechanism the energy transfer rate is independent of oscillator strength of the acceptor transition, which in the case of Ni^{2+}, we have measured to be ≈ 2–3 times less than for Co^{2+}.

Distinguishing between Förster and Dexter energy transfer is often not readily achieveable at short distances of interaction and has been little explored by comparing the fit of the fluorescence decay to the appropriate impulse responses. In contrast to eq. (8) describing Förster kinetics the equivalent expression for Dexter kinetics is of the form [30]

$$\phi/\phi_0 = \exp(-[A]/C_{AO}) \tag{10}$$

Hence the shape of ϕ/ϕ_0 vs. [A] provides, in theory at least, one method of distinguishing between the two kinetics.

3. Experimental

Perylene (Aldrich Gold Label), glycerol (Aldrich), $NiCl_2 \cdot 6H_2O$ (Aldrich) and $CrCl_3 \cdot 6H_2O$ (BDH) were used as received. $CoCl_2 \cdot 6H_2O$ (Merck p.a.) was recrystallized from methanol. L-α-dipalmitoylphosphatidylcholine (DPPC) was obtained from the Sigma Chemical Co.

Small unilammelar vesicles (SUV) were prepared using methanol injection at 328 K which is above the phase transition temperature for DPPC ($T_M = 314$ K). The lipid-to-probe ratio in all cases was 200:1. The concentration of the lipid in the buffer was 6.18×10^{-4} mol l^{-1}. The buffer solution was piperazine-*N*,*N*′-bis-2-ethane-sulfonic acid (PIPES) (Biochemical BDH) with KCl (Aldrich) and EDTA (Alrich). Sodium azide (Aldrich) was added to obtain a pH of 7 [31].

Fluorescence spectra were recorded with either a Perkin-Elmer MPF-44 E spectrofluorimeter with a quantum correction unit or a Shimadzu RF-540 spectrofluorimeter. Both instruments were fitted with a thermostated cuvette holder. All fluorescence spectra were corrected for reabsorption of the metal ion complexes, using the method of Marciniak [32].

Fluorescence decay kinetics were measured using the technique of time-correlated single photon counting [33]. Either the coaxial flashlamp filled with hydrogen or a Hamamatsu PLP-01 frequency doubled diode laser operated at 10 MHz repetition rate was used for excitation. Operating the lamp at 40 kHz gives an instrumental pulse ~ 1.5 ns FWHM. The diode laser gave an instrumental pulse width of ≈ 350 ps FWHM. The excitation wavelength for all measurements was 385 nm. Prism polarisers were used at the "magic angle" to eliminate rotational effects. The sample temperature was controlled by electrical heating (Eurotherm) with a precision of ±0.5 K. The maximum number of counts in a channel was between 1×10^4 and 2×10^4 recorded at channel

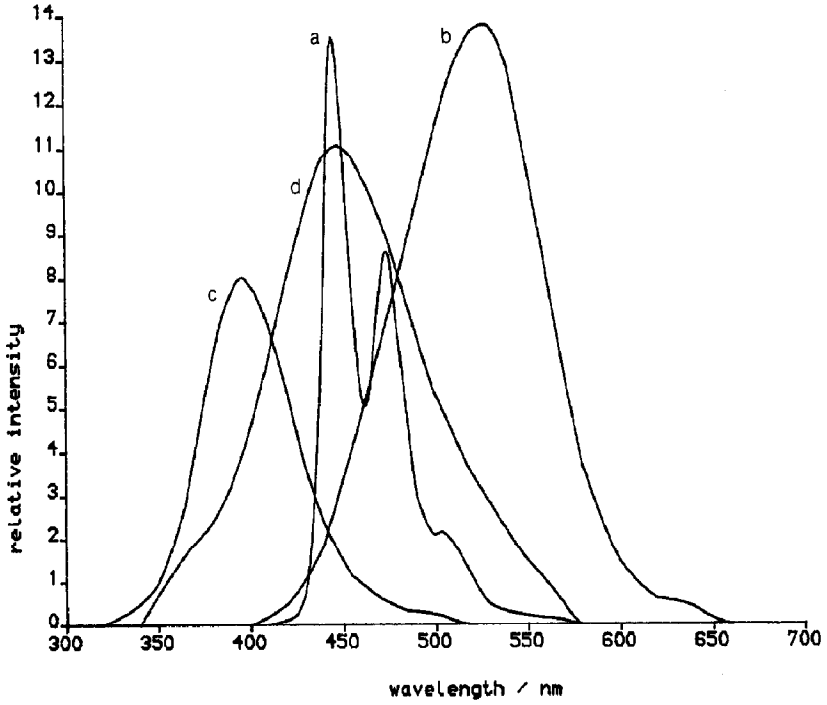

Fig. 1. Fluorescence spectrum for perylene in lipid bilayers (a) and the absorption spectra for Co^{2+} (b) and Ni^{2+} (c) ions bound to the lipid headgroup at $T = 303$ K, and for Cr^{3+} (d) ions in glycerol.

widths down to 84 ps/ch. Data analysis was performed using the IBH iterative reconvolution library.

4. Results and discussion

The fluorescence spectrum for perylene in DPPC bilayers and the absorption spectra for Co^{2+} and Ni^{2+} ions bound to the lipid headgroup at $T = 303$ K are shown in Fig 1. Also shown in Fig. 1 is the absorption spectrum for Cr^{3+} ions in glycerol which has the biggest overlap with the perylene fluorescence spectra. The Co^{2+} and Ni^{2+} absorption spectra can be seen to be on the low and high energy side of the perylene emission spectrum respectively. In the case of Ni^{2+} significantly more overlap with the perylene absorption is observed. Addition of metal ions to the vesicles did not affect their stability as a single phase transition at $T = 314$ K was observed at all metal ion concentrations.

In small unilamellar DPPC vesicles in the gel phase ($T = 303$ K) the fluorescence lifetime of perylene is 6.31 ns with a χ^2 of 1.31 and hence shows small deviations from a single exponential function. This we attributed to the effects of donor–donor energy transfer due to clustering of the perylene molecules in the gel phase [21]. The non-random distribution of probe molecules was observed in perylene concentration studies of the lipid bilayer [21] which showed no evidence for the formation of perylene dimers from the steady state spectra. Also, analysing the fluorescence decay at different emission wavelengths gave the same results confirming that perylene dimers are not formed and that the quenching mechanism is Förster type energy transfer. From these studies it was evident that the number of perylene molecules involved in the energy transfer processes is independent of the size of the perylene cluster once the minimum number of molecules were present for the donor–donor energy transfer process to occur [21]. When increasing the temperature to 323 K (i.e. the liquid crystalline phase), the fluorescence decay function can be fitted better to a monoexponential fit ($\chi^2 = 1.09$) with a reduced lifetime of 5.81 ns. In this phase the bilayer becomes more fluid and the volume is increased which results in the perylene molecule having more mobility and hence probe clustering will be reduced [34]. The fluorescence lifetimes measured here are in agreement with those reported in DMPC and DOPC vesicles [9,35].

4.1. Perylene–cobalt studies

When $CoCl_2 \cdot 6H_2O$ is added to the liposome suspension the fluorescence decay curves cannot be fitted to a monoexponential decay law. The deviations being significantly higher below the phase transition (T_M). The stronger quenching effect above T_M is evident from the faster fluorescence decay. At $[Co^{2+}] = 0.1$ mol l^{-1}, the mean lifetimes calculated from $\tau_e = \int_0^\infty tI(t)dt / \int_0^\infty I(t)dt$ are τ_e (303 K) = 3.80 ns and τ_e (323 K) = 3.29 ns. In the lipid bilayer the cobalt ions are anchored at the lipid headgroup with an

Table 1

Best-fit parameters at 303 K to a 3D Förster fit and values calculated for R_0 from eq. (4) for the fluorescence quenching of perylene at different Co^{2+}-ion concentrations in DPPC vesicles

Co^{2+} (mol l^{-1})	τ_0/ns	Förster kinetics 3D model parameter			Equation (4)	
		γ	χ^2_{3D}	R_0/Å	γ_A	R_0/Å
0.011	6.60 ± 0.21	0.138	1.25	17.7 ± 0.3	0.053	12.9 ± 1.0
0.021	6.45 ± 0.21	0.208	1.05	16.4 ± 0.2	0.123	13.8 ± 0.5
0.031	6.38 ± 0.24	0.299	1.22	16.3 ± 0.3	0.214	14.6 + 0.3
0.041	6.37 ± 0.24	0.352	1.13	15.7 ± 0.1	0.267	14.3 ± 0.3
0.060	5.95 ± 0.24	0.392	1.18	14.3 ± 0.1	0.307	13.2 ± 0.2
0.080	5.96 ± 0.27	0.430	1.23	13.4 ± 0.1	0.345	12.4 ± 0.2
0.100	6.15 ± 0.30	0.529	1.30	13.3 ± 0.1	0.444	12.6 + 0.2

ion-lipid binding constant for Co^{2+} and DPPC of 1.71 mol^{-1} [36]. Even at the lowest Co^{2+} concentration of 0.01 mol l^{-1} of cobalt chloride the Co^{2+} : lipid ratio is 12.5 : 1. Hence the metal ion concentration at the lipid headgroup is high.

Below the phase transition temperature (i.e. in the gel phase) diffusional effects are minimal, hence we have analysed the data in terms of Förster kinetics for both a three dimensional and a two dimensional representation. Intuitively a two dimensional model may appear to be more appropriate for the lipid system that we are studying given that the cobalt ions are bound to the lipid headgroup and the perylene molecules are within the interior of the bilayer. However, the χ^2 values are consistently better for the three-dimensional description and the values obtained for γ are similar for both models. Hence we have calculated values for the interaction radius, R_0, from eqs. (1) and (3) and these are given in Table 1. The values obtained for R_0 calculated for a two-dimensional model, are, within the error, the same as those calculated assuming a 3D system. Below T_M the values obtained for R_0 are not constant as expected but are too high at the low acceptor concentrations (i.e. for $[CoCl_2 \cdot 6H_2O] \leq 0.06$ mol l^{-1}). The value for R_0 calculated from the overlap of the absorption spectra of $CoCl_2 \cdot 6H_2O$ and the emission spectra of perylene using eq. (2) is 13.9 Å in the lipid bilayer and 12.4 Å in glycerol. The difference between the two values is due to the spectral shift of the Co^{2+} ion absorption. The experimental value for R_0 in glycerol solution is 13.4 Å [24]. Also, the plot of γ versus $[Co^{2+}]$ (Fig. 2) gives a value for R_0 of 12.1 ± 1.6 Å from the slope but does not go through the origin as predicted by eq. (3). This suggests that an additional energy transfer process is occurring at the low acceptor concentrations. This was found to be donor–donor energy transfer between the perylene molecules, as the rate of donor–donor energy transfer is comparable to the rate of donor–acceptor energy transfer [21]. Radiative energy transfer was excluded as no evidence was found for this in the steady state spectra. Analysing the perylene fluorescence decay with no quencher added in terms of Förster kinetics (eq. (1)) gave a

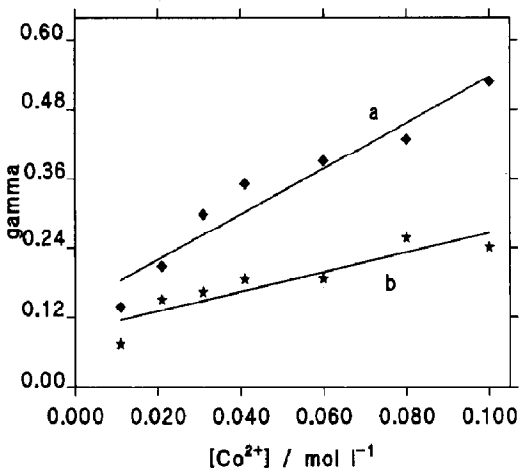

Fig. 2. Plot of γ vs. $[Co^{2+}]$ for perylene–cobalt energy transfer in lipid bilayers at (a) 303 K. and (b) 323 K.

value for γ_D of 0.120 ± 0.006 which is, within the error, consistent with the intercept of the straight line graph in Fig. 2 i.e. 0.140 ± 0.038. Given this value for γ_D we can analyse the fluorescence decays using eq. (4), which takes the effects of donor–donor energy transfer into account. The values obtained for R_0 (see Table 1) were then found to be constant with a mean value of 13.4 Å, in good agreement with the R_0 measured in glycerol and calculated from eq. (2).

Table 2 gives the parameters obtained when using Förster's model for a 3D system (eq. 1) to

Table 2

Best-fit parameters at 323 K to a 3D Förster fit and values calculated for R_0, taking donor–donor energy transfer into account, and D from eq. (5) for the fluorescence quenching of perylene at different Co^{2+}-ion concentrations in DPPC vesicles

Co^{2+} (mol l^{-1})	Förster kinetics 3D model parameters			R_0/Å	$D/10^{-6}$ cm^2 s^1
	τ_0/ns	γ	χ^2		
0.011	5.41±0.15	0.074	1.05	11.2±1.4	1.20±0.08
0.021	5.18±0.16	0.151	1.10	13.4±0.6	0.92±0.04
0.031	5.01±0.16	0.164	1.06	12.2±0.5	0.92±0.04
0.041	4.85±0.18	0.186	1.19	11.7±0.4	0.98±0.03
0.060	4.48±0.17	0.187	1.13	10.3±0.3	1.31±0.05
0.080	4.47±0.20	0.258	1.22	10.7±0.3	0.90±0.02
0.100	4.18±0.18	0.241	1.15	9.7±0.3	1.15±0.02

describe the fluorescence decay data above the phase transition temperature of the lipid. Once again the model of a 3D system was found to be more appropriate, as judged by the χ^2 values, but both the 2D and 3D models give similar γ and τ_0 values. Here the values obtained for τ_0 decrease significantly with increasing Co^{2+} concentration reflecting the diffusion of the perylene molecules and cobalt ions as might be expected in the liquid crystalline phase of the lipid bilayer. Below T_M the fluorescence lifetime, τ_0, is almost constant showing that little diffusion occurs in the gel phase (see Table 1).

We have therefore considered the expressions given by Gösele et al. [16,17] for diffusion controlled energy transfer (eqs. 5 and 6) in the liquid crystalline phase. To decide which is the more appropriate expression in our case we calculated r_F and r_{AD} from our experimental data. For $[Co^{2+}] = 0.061$ mol l^{-1}, we calculated $r_F = 8.6$ Å, from eqs. (5) and (7), and $r_{AD} = 4.4$ Å, from eq. (6), which then gives for the ratio r_F/r_{AD} a value of 1.95, indicating that eq. (5) is more appropriate and energy transfer dominates over diffusion. This is not the case in the solvent ethylene glycol where $r_F/r_{AD} < 1$ which shows that in this solvent the quenching of perylene fluorescence by cobalt ions is purely diffusion controlled as already reported [24].

The parameters obtained from interpreting the fluorescence decay data in the liposome above T_M, using eq. (5), are given in Table 2. The results show evidence for donor–donor energy transfer between the perylene molecules above the phase transition similar to that observed in the gel phase. When plotting γ versus $[Co^{2+}]$ the straight line graph does not go through the origin (Fig. 2). The critical transfer distance R_0 calculated from the gradient of this graph is 9.9 ± 1.8 Å which is less, although within the error of that observed below the phase transition where R_0 is calculated to be 12.1 ± 1.6 Å. Taking the data set with no quencher added and analysing in terms of Förster's model (eq. 1) gives $\gamma = 0055 \pm 0.006$ and $\tau_0 = 6.09$ ns. This γ value is close to the intercept of the graph in Fig. 2 (0.090 ± 0.029) consistent with the presence of donor–donor energy transfer above the phase transition.

Once again the occurrence of donor–donor energy transfer provides interesting evidence for there being clustering of the probe molecules. It is notable that this occurs above as well as below the phase transition. A 200:1 lipid-to-probe ratio corresponds to an equivalent molar concentration of $\approx 10^{-2}M$ and yet even in the same concentration in a homogeneous solution of perylene molecules, where self-absorption is the more predominant process, radiationless energy transfer between the perylene molecules is not evident as the fluorescence decays can be fitted well to a monoexponential fit albeit with an increased lifetime due to self absorption. However, this may not be surprising given that the mean separation between perylene molecules at this concentration is ≈ 55 Å and the Förster energy transfer radius is 35.7 Å [21]. This provides further supporting evidence for the non-random distribution of perylene molecules in the fluid phase of the bilayer. However, the perylene clusters need not be tightly bound in order for Förster energy transfer to occur. Indeed, the non-exponentiality of the fluorescence decay of other fluorophores in lipid bilayers, especially in the gel phase, may have their origin in inter fluorophore interactions such as energy transfer processes due to the non random distribution of fluorophores.

Above the phase transition the diffusion of both the donor and acceptor molecules as well as energy transfer from donor to donor and also acceptor presents a complex kinetic system. We should emphasise that in the treatment we are using the evidence points to donor–donor interactions appearing as two terms, namely Förster energy transfer as if static conditions prevailed and also diffusion of the donor sites. In such cases a diffusion term in the donor rate equation is also needed for describing the donor–donor energy transfer, this term not being required below the phase transition. Gochanour et al. [14] have derived an approximate expression to account for this behaviour in terms of the excitation diffusion coefficient, D_E, which is valid at long times and high donor concentrations and is given by

$$D_E = 0.428 C^{4/3} R_{0D}^2 \tau_0^{-1} \qquad (11)$$

where

$$C = \tfrac{4}{3}\pi[\mathrm{D}]N_{\mathrm{A}}R_{0\mathrm{D}}^{3} \quad (12)$$

This diffusion coefficient D_{E} forms part of the diffusion coefficient of the donor in eq. (5), the other part being due to translational diffusion. We can estimate D_{E} from the value obtained for [D] of 5.4×10^{-4} M which is calculated from the γ value obtained when no cobalt is present in the lipid bilayer above T_{M}. Calculated from the overlap integral (eq. 2) R_0 is 35.7 Å. This then gives a value for D_{E} of 0.22×10^{-6} cm^{-2} s^{-1}. This is less than the average value obtained for D of 1.06×10^{-6} cm s^{-1} from Table 2. The difference between these two values being due to the effect of translational diffusion which will also occur in the fluid phase of the bilayer. Translational diffusion (D_{T}) can be estimated from Stokes–Einstein theory if the viscosity of the medium is known. Above the phase transition the diffusion length ℓ_{dif} (= 11.4 Å) $\approx R_0$ so if we make the assumption that D_{T} is similar in the bilayer to that in ethylene glycol where ℓ_{diff} is also approximately equal to r_0 then $D_{\mathrm{T}} \approx 0.71 \times 10^{-6}$ cm^2 s^{-1} [24]. The sum of the two diffusion coefficients is then 0.93×10^{-6} cm^2 s^{-1} which is close to the average diffusion coeffient obtained in Table 2.

The R_0 values in Table 2 take donor–donor energy transfer into consideration and the average value for R_0 obtained is 11.3 Å which is less than the theoretical value of 13.9 Å. This discrepany is probably due to a difference in the local and bulk concentrations of Co^{2+} where the interfacial region is saturated with Co^{2+} ions. Hence increasing the amount of cobalt produces no further quenching of the perylene fluorescence with the result that the measured R_0 value still appears to slightly decrease with addition of cobalt. The values which we have obtained for R_0 and D demonstrate that this complex system can be reasonably modelled by a simple isotropic treatment to obtain sensible results.

The percentage of perylene molecules which are transferring energy to the cobalt ions can be estimated from the steady state spectra. Figure 3A shows plots of the relative fluorescence quantum yield ϕ_0/ϕ of perylene versus quencher concentration. Below and above T_{M} the plots show a negative departure from linear Stern–Volmer behaviour and exhibit the classic curvature associated with a fluorophore in environments with different susceptibilities to the quencher [1] rather than the positive curvature associated with Förster quenching. Figure 3B shows the straight line graph obtained when analysing the data with the following eq. [1]:

$$\frac{I_0}{\Delta I} = \frac{1}{f_{\mathrm{a}}K[\mathrm{A}]} + \frac{1}{f_{\mathrm{a}}} \quad (13)$$

where $\Delta I = I_0 - I$, f_{a} is the fraction of the probe molecules involved in Förster energy transfer to

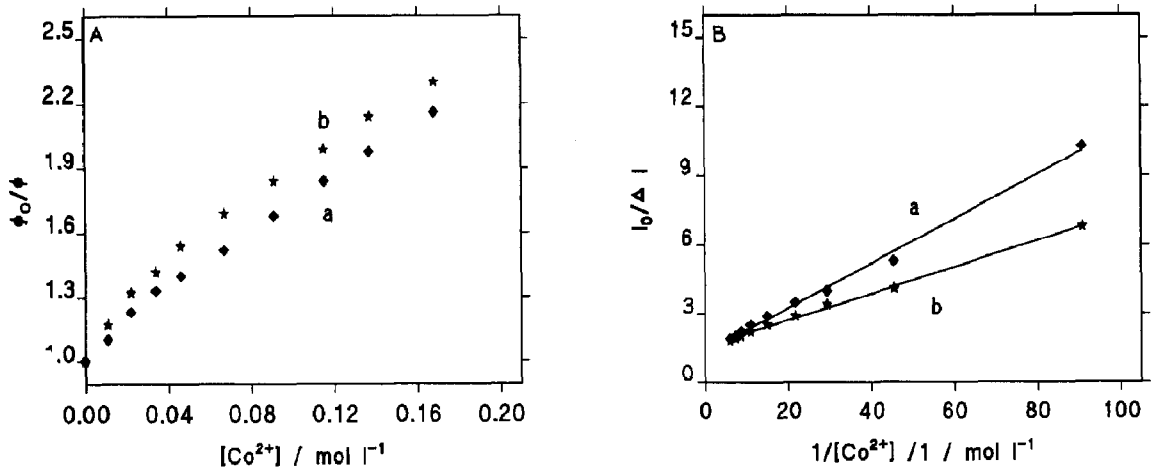

Fig. 3. (A) Stern–Volmer plot for the quenching of the perylene fluorescence by Co^{2+} ions in DPPC vesicles at (a) 303 K and (b) 323 K. (B) Modified Stern–Volmer plot from eq. (13) at (a) 303 K and (b) 323 K.

the metal ion and K is a quenching constant (analogous to Stern–Volmer) associated with this fraction. From Fig. 3B, f_a is $76.0 \pm 11.6\%$ for the gel phase and $64.6 \pm 4.0\%$ for the liquid crystalline phase. These percentages are, within the error, the same. We can therefore conclude that $\approx 70\%$ of the perylene molecules are transferring energy to the cobalt ion and the remaining 30% are either isolated sites of perylene molecules or involved in donor–donor energy transfer that is not eventually quenched by the cobalt ion. In the case of the lipid bilayer the perylene molecules can either be isolated or in a cluster and the cobalt ions will either be bound or close to the polar headgroup of the lipid molecules. The perylene molecules in the centre of the cluster are more likely to transfer energy to other perylene molecules as opposed to the cobalt ion. The diminishing effect on quenching observed when increasing the Co^{2+} concentration i.e. ϕ/ϕ_0 levels off is due to saturation in the extent of Förster quenching by Co^{2+}.

4.2. Perylene–nickel studies

Table 3 gives the parameters obtained using a 2D Förster model for nickel quenching of perylene fluorescence both below and above the phase transition. Once again there is evidence for donor–donor energy transfer from a plot of γ versus $[Ni^{2+}]$ where the straight line does not go through the origin. Also given in Table 3 is the calculated values for R_0 taking into account perylene–perylene energy transfer. The average value calculated for R_0 is the same below and above the phase transition and is 7.4 Å. This value is less than that calculated from eq. (2) of 9.4 Å. Also, as can be seen from the table the values calculated for R_0 systematically decrease with increasing Ni^{2+} concentration. This may again be due to the saturation effect where increasing $[Ni^{2+}]$ leads to no further quenching of the perylene fluorescence. A number of other discrepancies are evident with both the predictions of the Förster model and the Co^{2+} results shown in Tables 1 and 2. In particular τ_0 for Ni^{2+} quenching below T_M is anything but constant and systematically decreases with increasing $[Ni^{2+}]$. It is

Table 3

Kinetic parameters obtained from the analysis using 2D Förster kinetics for the fluorescence quenching of perylene by Ni^{2+} ions in DPPC vesicles at 303 K and 323 K and a lipid-to-probe ratio of 358:1

Ni^{2+} (mol l^{-1})	τ_0 (ns)	γ	χ^2	R_0 (Å)
T = 303 K				
0.033	6.66 ± 0.06	0.130	1.14	8.5
0.068	6.44 ± 0.07	0.151	1.24	7.6
0.106	6.31 ± 0.07	0.181	1.10	7.4
0.137	6.17 ± 0.08	0.214	1.31	7.5
0.174	6.00 ± 0.07	0.246	1.05	7.5
0.209	5.95 ± 0.07	0.257	1.03	7.2
0.253	5.79 ± 0.07	0.306	1.16	7.8
0.285	5.79 ± 0.07	0.309	1.17	7.0
0.321	5.56 ± 0.07	0.333	1.08	7.0
0.353	5.61 ± 0.07	0.316	1.19	6.6
T = 323 K				
0.033	5.98 ± 0.07	0.078	1.46	8.1
0.068	5.87 ± 0.06	0.109	1.16	7.7
0.106	5.71 ± 0.06	0.128	1.22	7.2
0.137	5.65 ± 0.06	0.161	1.14	7.4
0.174	5.48 ± 0.06	0.221	1.13	7.8
0.209	5.46 ± 0.07	0.227	1.18	7.4
0.253	5.31 ± 0.07	0.266	1.16	7.4
0.285	5.28 ± 0.07	0.263	1.20	7.1
0.321	5.19 ± 0.07	0.287	1.05	7.0
0.353	5.14 ± 0.06	0.262	1.17	6.6

extremely unlikely that this is due to collisional quenching because of the low fluidity of the gel phase. Above the phase transition, the values obtained for τ_0 do not decrease as rapidly with increasing Ni^{2+} concentration compared to that observed for Co^{2+} quenching. Indeed the slope obtained for a plot of τ/τ_0 vs. $[Ni^{2+}]$ is within the error the same both above and below the phase transition indicating that diffusional quenching is not the most dominant mechanism above T_M in contrast to that observed for Co^{2+} quenching. In addition, for Ni^{2+} quenching the 2D Förster model gives a slight improvement over the 3D model although there was little difference in the τ_0 and γ values, whereas with Co^{2+} the opposite was true [37]. Figure 4 shows a 2D Förster fit to the data set with 0.209 mol l^{-1} of Ni^{2+} added below the phase transition.

The Stern–Volmer plot in Fig. 5 of ϕ_0/ϕ for perylene in DPPC at 303K and 323K quenched

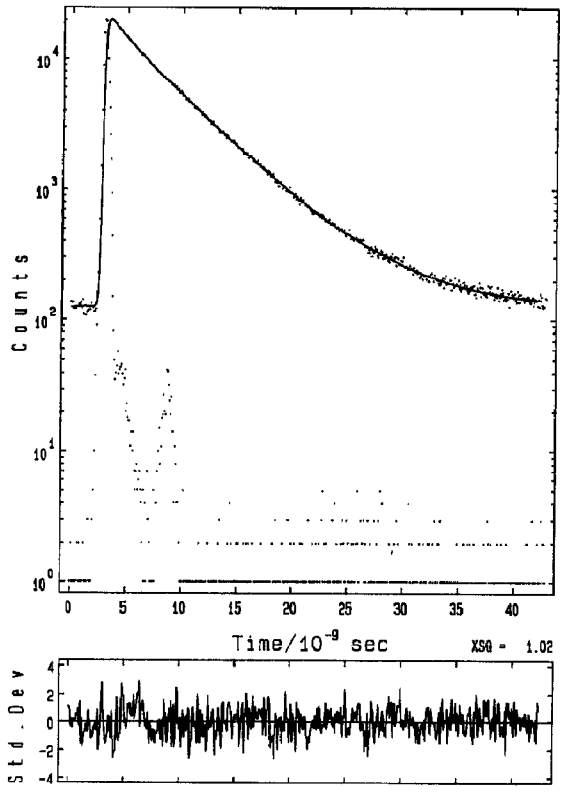

Fig. 4. 2D Förster fit to 358:1 DPPC:perylene quenched by 0.209 mol l^{-1} of Ni^{2+} at 303 K using diode laser excitation. Decay parameters obtained are given in Table 3.

by Ni^{2+} shows a slight positive curvature as is expected for quenching via the Förster energy transfer mechanism but is in sharp contrast to the

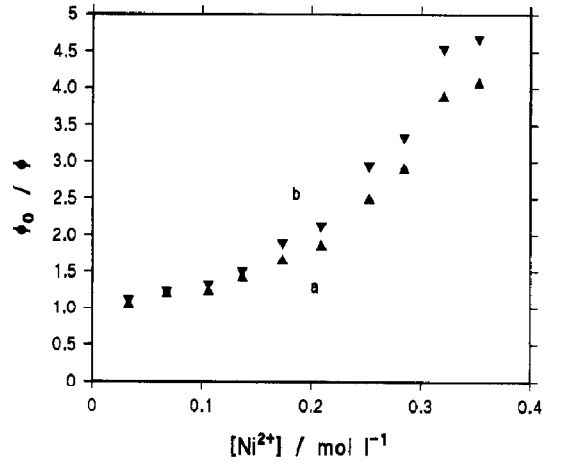

Fig. 5. Stern–Volmer plots for the quenching of the perylene fluorescence by Ni^{2+} ions at (a) 303 K and (b) 323 K.

negative curvature for quenching with Co^{2+}. When this behaviour is combined with the results of the time-resolved analysis there is good evidence that, although the Förster model provides a good decay-curve parameterisation, a different quenching mechanism is dominant for Ni^{2+} in lipid bilayers. We thus investigated the behaviour of perylene fluorescence quenching by Ni^{2+} in undiluted glycerol, a solvent in which the Förster model had proved correct for Co^{2+} quenching [24]. All samples in this case were degassed. Here evidence was found for a different quenching mechanism other than Förster dipole–dipole energy transfer. In a plot of γ vs. $[Ni^{2+}]$ the curves do not pass through zero which places the application of the Förster model in doubt. However, R_0 calculated from the gradient of the graph is 8.28 Å which is close to the theoretical value of 9.1 Å from eq. (2). The offset from zero observed here must be due to an additional quenching mechanism which in this case cannot be donor–donor energy transfer as no perylene clustering is observed in a homogeneous solution of 5×10^{-6} mol l^{-1} concentration.

The evidence presented so far is strongly against the perylene–Ni^{2+} interaction being solely Förster type, without pointing towards another source of quenching mechanism. At present the most likely alternative looks to be that of either electron transfer or Dexter exchange interaction. The direct evidence for the latter is shown in Fig 6 where ϕ/ϕ_0 and τ/τ_0 are plotted vs. $[Ni^{2+}]$. A fit to the ϕ/ϕ_0 data using the Förster mechanism, eq. (8), is poor and results in an R_0 value of 14.2 Å which is too high. Fitting using the exponential curvature predicted by the Dexter mechanism, eq. (7), gives a much better fit over all the data. However, we were unsuccessful in fitting the time resolved data to the Dexter decay function [38]. We are currently investigating the possibility that the quenching kinetics observed here are a combination of the two mechanisms.

4.3. Perylene–chromium studies

For comparison with the results presented so far, the quenching of perylene fluorescence by Cr^{3+} ions was investigated in the viscous solvent

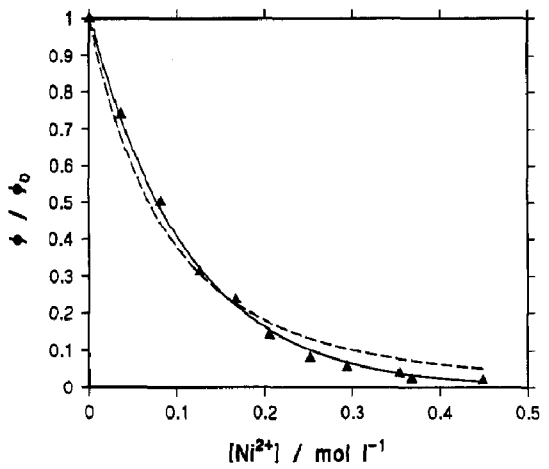

Fig. 6. Stern–Volmer plots for perylene fluorescence quenched by Ni^{2+} in glycerol at 25°C. ϕ/ϕ_0 is fitted to both Förster (dashed line) and Dexter (solid line) mechanisms.

glycerol. The interaction radius for perylene to Cr^{3+} energy transfer is 16.7 Å from eq. (2). Table 4 gives the parameters obtained when fitting to the Förster function for 3D energy transfer, which resulted in less than ideal fits as judged by the χ^2 values and the residuals. Nevertheless, R_0 calculated from the γ values obtained and eq. (3) gave a reasonably close estimate for R_0 of 17.5 Å and τ_0 is independent of $[Cr^{3+}]$. A similar trend to that observed for Ni^{2+} was found in a plot of γ vs. $[Cr^{3+}]$, where once again the straight line did not pass through the origin. In this case a fit to the steady state data, i.e. a plot of ϕ/ϕ_0 vs. $[Cr^{3+}]$, found a good fit to the Förster mechanism—eq. (8)—but found an R_0 value of 22.4 Å which is much higher than that predicted by eq. (2). This also indicates an alternative form of quenching in addition to or in place of Förster type energy transfer. However, in this case Dexter electron exchange is not a possibility as the interaction distance is too large (i.e. > 10 Å).

Table 4

Kinetic parameters obtained from the analysis using 3D Förster kinetics for the fluorescence quenching of perylene by Cr^{3+} ions in glycerol at 296 K

$[Cr^{3+}]$ (mol l^{-1})	τ_0 (ns)	γ	χ^2
0.001	4.93 ± 0.03	0.041	1.19
0.004	4.95 ± 0.09	0.082	1.16
0.005	4.92 ± 0.09	0.086	1.04
0.007	4.94 ± 0.10	0.114	1.28
0.013	5.06 ± 0.12	0.193	1.43

Table 5

Values for R_0 (Å) obtained from eq. (2), steady state and time-resolved measurements for energy transfer from perylene to metal ions in glycerol at 296 K

Principle used	Co^{2+}	Ni^{2+}	Cr^{3+}
Theory eq. (2)	12.4	9.15	16.7
Time resolved measurements	13.4	8.28	17.5
Steady state measurements	12.7	14.2	22.4

5. Conclusions

In summarising the results we have obtained so far, Table 5 gives the values obtained for R_0 for perylene energy transfer to the transition metal ions we have studied in glycerol. In the case of the cobalt ion good agreement between theory (eq. 2), steady state and time resolved data for the value of R_0 is obtained. This provides self-consistent evidence that perylene fluorescence quenched by cobalt ions exhibits classic Förster dipole-dipole energy transfer. Quenching by nickel and chromium ions does not exhibit such a self-consistent trend. Here the R_0 values obtained from time-resolved measurements agree well with that obtained from eq. (2) while the values obtained from the steady state fluorescence data are too high. This indicates that an additional form of fluorescence quenching is observed as well as Förster type energy transfer, the presence of this additional mechanism only being reflected in the time resolved data as poorer χ^2 values. For Ni^{2+} ions the additional mechanism could be that of Dexter electron exchange interaction. Also, the redox potentials indicate that electron transfer is possible between perylene and Ni^{2+} and Cr^{3+} ions, whereas for Co^{2+} ions this is not the case.

Energy transfer from perylene to cobalt ions has been demonstrated to be classic Förster type energy transfer in lipid bilayers. Donor–donor energy transfer between perylene molecules due to clustering effects is shown to occur both above and below the main phase transition of the lipid. Once this effect has been accounted for, the transfer of energy from the perylene molecules to

the cobalt ions is shown to follow Förster kinetics in the gel phase and simple three-dimensional diffusion theory in the liquid crystalline phase. In lipid bilayers the perylene fluorescence quenching by Ni^{2+} ions does not exhibit classic Förster energy transfer but shows evidence for an additional mechanism. Another interesting feature observed for Ni^{2+} quenching above T_M in the lipid bilayer is the lack of diffusional quenching observed. Given the differences in the quenching mechanisms observed time-resolved fluorescence quenching techniques may prove to be more useful in studying the diffusion of metal ions in membrane systems than the complexity of such systems would at first indicate. Further work is at present underway to understand the complicated fluorescence quenching kinetics between fluorophores and transition metal ions both in solution and heterogeneous systems. Once an understanding of such kinetics has been established further applications may follow. For example, we have recently demonstrated a metal ion sensor based on interfacial Förster energy transfer from perylene to Co^{2+} ions across a Nafion polymer membrane [39].

Acknowledgement

We wish to thank the SERC for financial support.

References

1 J.R. Lakowicz, Principles of fluorescence spectroscopy, (Plenum Press, New York, 1983).
2 J.A. Kemlo and T.M. Shepherd, Chem. Phys. Lett. 47 (1977) 158.
3 M.J. Aguirre, E.A. Lissi and A.F. Olea, J. Photochem. 36 (1987) 177.
4 T. Nakamura, A. Kira and M. Imamura, J. Phys. Chem. 86 (1982) 3359.
5 J. Jay, L.J. Johnston and J.C. Scaiano, Chem. Phys. Lett 148 (1988) 517.
6 K. Kalyanasundaram, Photochemistry in microheterogeneous systems, ch. 2 and references therein (Academic Press, New York, 1987).
7 R. Konuk, J. Cornelisse and S.P. McGlynn, J. Phys. Chem. 93 (1989) 7405.
8 M.D. Barkley, A. Kowalczyk and L. Brand, J. Chem. Phys. 75 (1981) 3581.
9 J.R. Lakowicz and J.R. Knutson, Biochemistry 19 (1980) 905.
10 Th. Förster Z. Naturforsch. 4a (1949) 321.
11 D.L. Huber Phys. Rev. B. 20 (1979) 2307.
12 D.L. Huber Phys. Rev. B. 20 (1979) 5333.
13 M. Yokota and O. Tanimoto, J. Phys. Soc. Jpn. 22 (1967) 779.
14 C.G. Gochanour, H.C. Anderson and M.D. Fayer J. Chem. Phys. 70 (1979) 4254.
15 R.F. Loring, H.C. Anderson and M.D. Fayer J. Chem. Phys. 76 (1982) 2015.
16 U. Gösele, M. Hauser, U.K.A. Klein and R. Frey, Chem. Phys. Lett. 34 (1975) 519.
17 U.K.A. Klein, R. Frey, M. Hauser and U. Gösele, Chem. Phys. Lett. 41 (1976) 139.
18 A.I. Burshtein, J. Luminesc. 34 (1985) 201.
19 S.G. Fedorenko and A.I. Burshtein, Chem. Phys. 98 (1985) 341.
20 K.K. Pandey, H.C. Joshi and T.C. Pant Chem. Phys. Lett. 148 (1988) 472.
21 A.S. Holmes, D.J.S. Birch, K. Suhling, R.E. Imhof, T. Salthammer and H. Dreeskamp Chem. Phys. Lett. 186 (1991) 189.
22 N. Tamai, T. Yamazaki, I. Yamazaki and N. Mataga, Chem. Phys. Lett. 120 (1985) 24.
23 K.K. Pandey and T.C. Pant Chem. Phys. Lett. 170 (1990) 244.
24 T. Salthammer, H. Dreeskamp, D.J.S. Birch and R.E. Imhof J. Photochem. Photobiol. A: Chemistry 55 (1990) 53.
25 A.G.E. Läufer, H. Dreeskamp and K.A. Zachariasse, Chem. Phys. Lett. 121 (1985) 523.
26 H. Dreeskamp, A. Läufer and M. Zander, Chem. Phys. Lett. 112 (1984) 479.
27 L. Stryer, Annu. Rev. Biochem. 47 (1978) 819.
28 R.E. Dale, J. Eisinger and W.E. Blumberg, 26 (1979) 161.
29 D.L. Dexter, J. Chem. Phys. 21 (1953) 836.
30 V. Breuninger and A. Weller, Chem. Phys. Lett. 23 (1973) 40.
31 L.K. Bar, Y. Barenholz and T.E. Thompson, Biochemistry 26 (1987) 5460.
32 B. Marciniak, J. Chem. Edu. 63 (1986) 998.
33 D.J.S. Birch and R.E. Imhof, in: Topics in fluorescence spectroscopy, vol. 1: Techniques, ed. J.R. Lakowicz (Plenum Press, New York, 1991) p. 1.
34 D.J.S. Birch, A.S. Holmes, R.E. Imhof and J. Cooper, Chem. Phys. Lett. 148 (1988) 435.
35 P.L.-G. Chong, B.W. v.d. Meer and T.E. Thompson, Biochim. Biophys. Acta 813 (1985) 253.
36 G. Cevc and D. Marsh, Phospholipid bilayers (Wiley, New York 1987).
37 D.J.S. Birch, K. Suhling, A.S. Holmes, T. Salthammer and R.E. Imhof, SPIE Proc. 1640 (1992) 707.
38 H. Inokuti and F. Hirayama, J. Chem. Phys. 43 (1965) 1978.
39 A. Sanderson, A.S. Holmes, D. McLoskey, D.J.S. Birch and R.E. Imhof, SPIE Proc. 1885 (1993) 466.